

Supplementary Information

**Multi-electron redox phenazine for ready-to-charge  
organic batteries**

Minah Lee<sup>a†‡</sup>, Jihyun Hong<sup>b†</sup>, Byungju Lee<sup>b</sup>, Kyojin Ku<sup>b</sup>, Sechan Lee<sup>b</sup>, Chan Beum Park<sup>a\*</sup>,  
Kisuk Kang<sup>b,c\*</sup>

<sup>a</sup>*Department of Materials Science and Engineering, KAIST, 291 Daehak-ro, Yuseong-gu, Daejeon  
34141, Republic of Korea*

<sup>b</sup>*Department of Materials Science and Engineering, Research Institute of Advanced Materials (RIAM),  
Seoul National University, 1 Gwanak Road, Seoul 151-742, Republic of Korea*

<sup>c</sup>*Center for Nanoparticle Research, Institute for Basic Science (IBS), Seoul National University 1  
Gwanak Road, Seoul 151-742, Republic of Korea*

<sup>†</sup>These authors contributed equally to this work. \*e-mail: parkcb@kaist.ac.kr; matlgen1@snu.ac.kr.

## 1. Computational details

Density functional theory (DFT) based calculations were conducted for geometry optimization, energy evaluation, and vibration mode prediction of the molecules, using Gaussian 09 quantum chemistry package.<sup>2</sup> Spin-unrestricted calculations were performed based on the Becke–Lee–Yang–Parr (B3LYP) hybrid exchange-correlation functional<sup>3-5</sup> and triple-zeta valence polarization (TZVP) basis set.<sup>6-7</sup> The solvation of TEGDME were implicitly considered with applying dielectric constant of 7.9. Atomic charge was calculated using Mulliken population.<sup>8</sup> HOMO density was calculated with CUBEGEN utility embedded in Gaussian 09, and visualized with Materials Studio package.

## 2. Supplementary discussions

### 2.1. Ex situ spectroscopic analyses on DMPZ electrode (Figure 3)

We examined the structural change in the DMPZ electrode during the battery operation using UV/Vis absorption spectroscopy (Figure 3b). The as-prepared electrode exhibited the characteristic peak of DMPZ at 336 nm.<sup>9</sup> However, when the electrode was half-charged (HC) by one-electron oxidation, two separate absorption bands were observed at 350 and 450 nm, which may have originated from radical cations.<sup>10-11</sup> When fully charged (FC), the absorption of 350 nm red-shifted further to 370 nm. As the electrode was discharged, the absorption returned to the previous state. The absorption of the half-discharged state (HD) corresponded well to the absorption of the HC state, and the absorption of the fully discharged state recovered the original absorption state at rest, confirming the reversibility and stability of the redox reaction.

To trace the electron transfers in DMPZ molecules during the electrochemical reactions, we performed *ex situ* analyses on electrodes cycled in TEGDME electrolyte with LiTFSI using spectroscopic tools. The X-ray photoelectron spectroscopy (XPS) scans in Figure S2c reveal the reversible redox reaction around nitrogen atoms in the pyrazine ring of DMPZ during battery cycling, as proposed in Figure 1a. In the N 1s spectra, the peak centered at 399.7 eV of the as-prepared electrode shifted to higher energy ( $\Delta E = \sim 1$  eV) during the charge and then returned to the initial position. This finding is attributed to the reversible conversion of non-conjugated  $sp^3$  -NC- groups into conjugated  $sp^3$  -NC- groups, suggesting that the nitrogen atoms are redox-active centers. The reversible change in the C 1s spectra was also observed (Figure 3d). For the as-prepared electrode, the C 1s spectrum was deconvoluted into five peaks with full-width at half-maximum values of 1.0 eV, corresponding to carbon atoms within -C-C-

bonds in conductive agent (284.5 eV), methyl groups (284.9 eV), -H-C-C- bonds in benzene (ring I/III, 285.2 eV, 285.6 eV), and -C-N-C- in pyrazine (ring II, 286.2 eV) motifs of DMPZ, respectively (Figure S2).<sup>12-14</sup> The peaks for -H-C-C- bonds (285.2 eV, 285.6 eV) and -C-N-C- bonds (286.2 eV) indicated a reversible shift along the state of the charge; however, the degree of shift was much less than for nitrogen. In our DFT calculations on the DMPZ molecules at different states of charge, the variation of electron density in carbon and nitrogen atoms was consistent with the XPS results (Figure S3). For the pristine state, the calculations revealed the presence of four different electron densities of carbon atoms. As the electrons were extracted from the DMPZ, the charge density varied most significantly at the nitrogen atoms followed by the carbon atoms in the heterocyclic system except for the methyl groups, which agrees well with the XPS results. The degree of variation in the charge density at nitrogen atoms was, however, less than previously reported for n-type flavin<sup>[11, 28]</sup> and pteridine<sup>[13]</sup> systems, where the inserted electrons are localized in the diazabutadiene motif, which plays the roles of both the redox center and lithium acceptor. In the p-type (anion-associating) DMPZ molecules, the electrons were observed to be rather delocalized in the heterocyclic system.

The evolution of the molecular structure of DMPZ during the electrochemical reactions was verified using *ex situ* Fourier-transform infrared (FTIR) spectroscopy (Figure 3e). According to the vibrational modes, the FTIR spectra of the as-prepared electrode can be divided into three regions that represent (i) stretching of C-H bonds in a heterocyclic system and methyl groups (3800–3100 cm<sup>-1</sup>), (ii) stretching of C=C and C-N-C bonds (1700–1250 cm<sup>-1</sup>), and (iii) bending of C-H bonds in a heterocyclic system and methyl groups (1200–1000 cm<sup>-1</sup>). The vibrational mode of each peak was determined using DFT calculations, and the results are listed in Supporting Table 2. As the DMPZ//Li cells were charged and discharged, the characteristic FTIR spectra reversibly evolved and were restored. Most peaks observed in the rest state

(3405–3575, 1615, 1476, 1360, 1277, and 1147  $\text{cm}^{-1}$ ) gradually disappeared during charge and then recovered by the discharge. We attribute the dramatic change of the spectra to the delocalized electrons in the heterocyclic system of DMPZ during the redox reactions, which increase the electron densities of most atoms in heterocyclic systems, affecting their vibrational modes. Nevertheless, the most noticeable change was observed for the vibrational modes of stretching of C=C and C-N-C bonds in the heterocyclic system, where a sharp peak was evolved at 1550  $\text{cm}^{-1}$  during the charge, indicating that the nitrogen atoms in the pyrazine ring are the redox center. The FTIR spectra fully recovered during the following discharge, indicating that the structural evolution of DMPZ is highly reversible and stable at the molecular level.

### 3. Supplementary figures

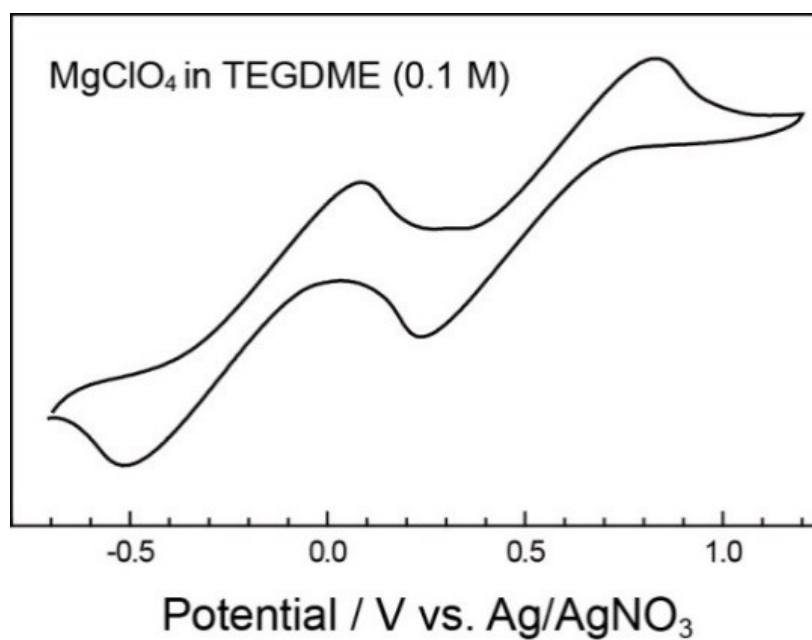


**Figure S1.** Cyclic voltammetry of DMPZ in 0.1 M MgClO<sub>4</sub>/TEGDME electrolyte. Reversible two-step redox reactions of DMPZ was observed with large polarization due to the low ionic conductivity of electrolytes originated from the strong solvation between ions and solvents.

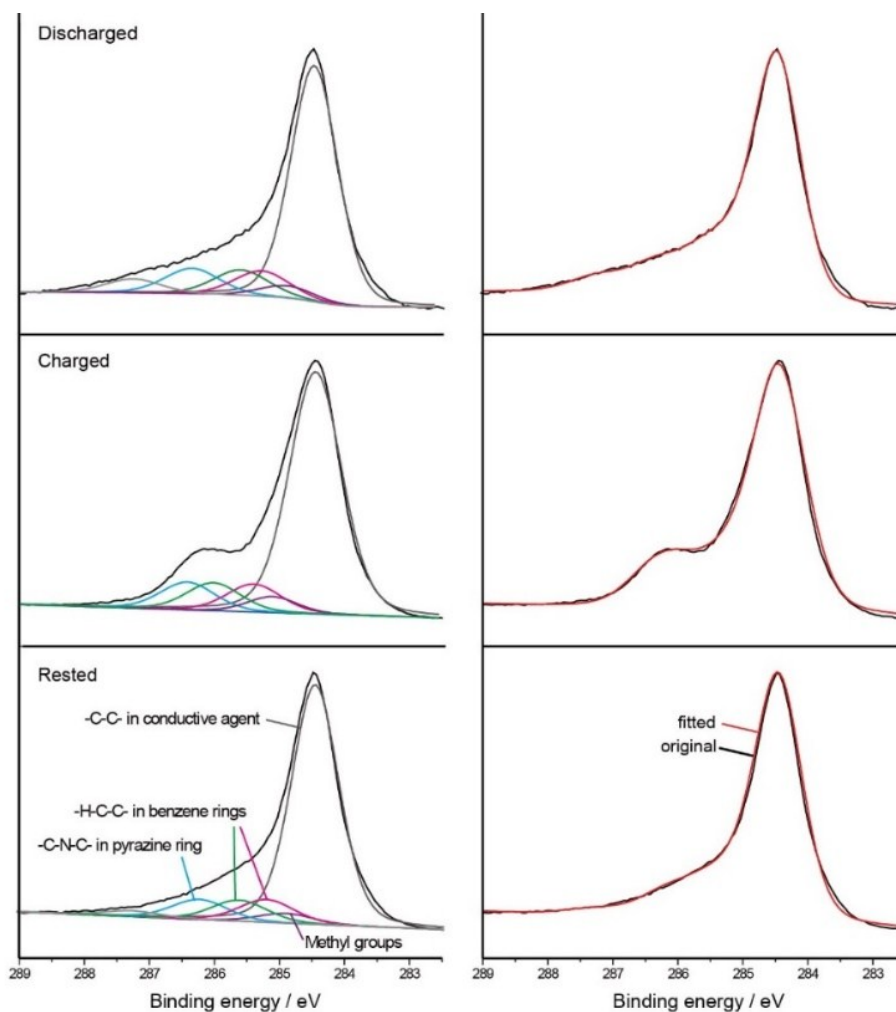


**Figure S2.** Deconvolution results of XPS local C 1s spectra of DMPZ electrodes at different state of charge. Reversible upshift and recovery of binding energy was observed for the peaks from the active compounds, which indicates the redistribution of electrons in the DMPZ molecule during the electrochemical cycling.

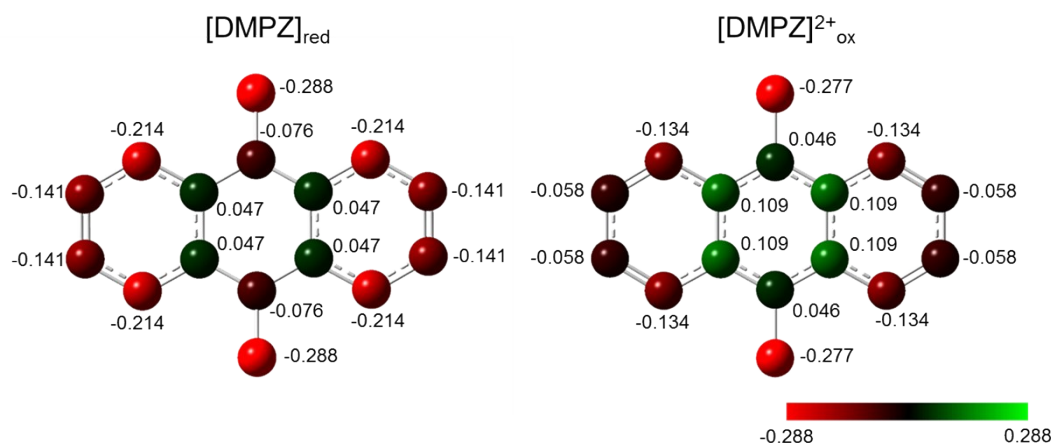


**Figure S3.** Mulliken charge population of DMPZ molecules obtained by DFT calculations. The most significant change of electron density was observed in pyrazine ring (ring II), which suggests that the conjugated diazabutadiene motif is the redox center.

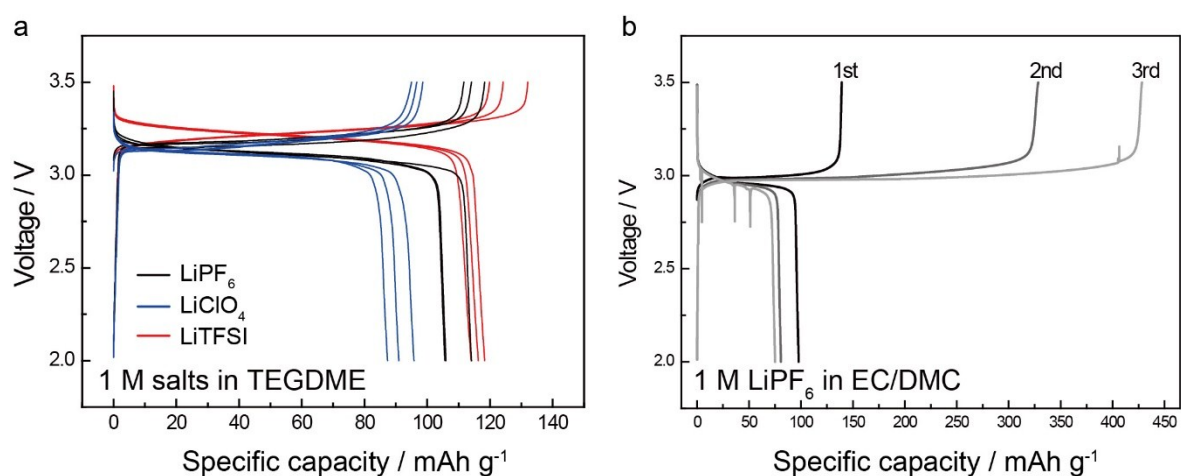


**Figure S4.** Charge/discharge profiles of DMPZ for initial three cycles within a voltage range of 3.5-2.0 V (vs. Li) in different electrolytes. a) 1 M  $\text{LiPF}_6$  (black),  $\text{LiClO}_4$  (blue), and  $\text{LiTFSI}$  (red) in TEGDME electrolytes, and b) 1 M  $\text{LiPF}_6$  in EC/DMC electrolyte. The high charge capacity beyond the theoretical capacity of DMPZ, and low reversible discharge capacity suggest a possible shuttle reaction of DMPZ due to its high solubility in carbonate-based electrolytes with high dielectric constants.

**Table S1.** Redox potentials of DMPZ in various electrolytes. The irreversible oxidation of  $[\text{DMPZ}]^+_{\text{rad}}$  in solvents with high donor number is attributed to the demethylation of DMPZ, which results in the formation of 5-methylphenazinium-type products.

Solvent (Donor number)	Redox potential (mV vs. Ag/AgNO <sub>3</sub> )					
	$E_{\text{c}}^{\text{red/rad}}$	$E_{\text{a}}^{\text{red/rad}}$	$E_{1/2}^{\text{red/rad}}$	$E_{\text{c}}^{\text{rad/ox}}$	$E_{\text{a}}^{\text{rad/ox}}$	$E_{1/2}^{\text{rad/ox}}$
ACN (14.1)	-212	-130	-171	502	598	550
TEGDME (16.6)	-210	-145	-178	350	426	388
DMF (26.6)	-225 (-300)*	-145 (-250)*	-185 (-275)*	-	504	-
DMSO (29.8)	-280 (-385)*	-186 (-297)*	-238 (-341)*	-	434	-

\*Redox potential of shoulder peaks originated from demethylation of DMPZ molecules.

**Table S2.** Peak assignments in FTIR spectrum. The reversible changes of the vibrational modes were observed to be most dominant for the stretching of C=C and C-N-C bonds (Region 2 in Figure 3e) in the heterocyclic system.

Wavenumber (cm <sup>-1</sup> )	Vibrational mode	Region in Figure 3d
3405 ~ 3575	Asymmetrical stretching of C-H bonds in methyl groups In-plane asymmetrical stretching of C-H bonds in ring I and III	Region 1
1615	In-plane asymmetrical stretching of C=C bonds in ring I and III In-plane symmetrical stretching of C=C bonds in ring I and III	Region 2
1476	In-plane symmetrical stretching of C=C bonds in ring II In-plane asymmetrical stretching of C-N-C bonds in ring II	
1360	In-plane asymmetrical stretching of C-N-C bonds in ring II	
1277	In-plane symmetrical stretching of C=C bonds in ring I, II and III In-plane symmetrical stretching of C-N-C bonds in ring II	
1147	Rocking of methyl groups In-plane bending of H-C=C-H in ring I and III	Region 3

## References

1. Terada, E.; Okamoto, T.; Kozaki, M.; Masaki, M. E.; Shiomi, D.; Sato, K.; Takui, T.; Okada, K., *J. Org. Chem.* **2005**, *70* (24), 10073-10081.
2. Frisch, M. J.; Trucks, G. W.; Schlegel, H. B.; Scuseria, G. E.; Robb, M. A.; Cheeseman, J. R.; Scalmani, G.; Barone, V.; Mennucci, B.; Petersson, G. A.; Nakatsuji, H.; Caricato, M.; Li, X.; Hratchian, H. P.; Izmaylov, A. F.; Bloino, J.; Zheng, G.; Sonnenberg, J. L.; Hada, M.; Ehara, M.; Toyota, K.; Fukuda, R.; Hasegawa, J.; Ishida, M.; Nakajima, T.; Honda, Y.; Kitao, O.; Nakai, H.; Vreven, T.; Montgomery Jr., J. A.; Peralta, J. E.; Ogliaro, F.; Bearpark, M. J.; Heyd, J.; Brothers, E. N.; Kudin, K. N.; Staroverov, V. N.; Kobayashi, R.; Normand, J.; Raghavachari, K.; Rendell, A. P.; Burant, J. C.; Iyengar, S. S.; Tomasi, J.; Cossi, M.; Rega, N.; Millam, N. J.; Klene, M.; Knox, J. E.; Cross, J. B.; Bakken, V.; Adamo, C.; Jaramillo, J.; Gomperts, R.; Stratmann, R. E.; Yazyev, O.; Austin, A. J.; Cammi, R.; Pomelli, C.; Ochterski, J. W.; Martin, R. L.; Morokuma, K.; Zakrzewski, V. G.; Voth, G. A.; Salvador, P.; Dannenberg, J. J.; Dapprich, S.; Daniels, A. D.; Farkas, Ö.; Foresman, J. B.; Ortiz, J. V.; Cioslowski, J.; Fox, D. J. *Gaussian 09*, Gaussian, Inc.: Wallingford, CT, USA, 2009.
3. Lee, C.; Yang, W.; Parr, R. G., *Phys. Rev. B* **1988**, *37* (2), 785-789.
4. Becke, A. D., *J. Chem. Phys.* **1993**, *98* (7), 5648-5652.
5. Stephens, P. J.; Devlin, F. J.; Chabalowski, C. F.; Frisch, M. J., *J. Phys. Chem.* **1994**, *98* (45), 11623-11627.
6. Schäfer, A.; Huber, C.; Ahlrichs, R., *J. Chem. Phys.* **1994**, *100* (8), 5829-5835.
7. Klaumünzer, B.; Kröner, D.; Saalfrank, P., *J. Phys. Chem. B* **2010**, *114* (33), 10826-10834.
8. Mulliken, R. S., *J. Chem. Phys.* **1955**, *23* (10), 1833-1840.
9. Schuster, G. B.; Schmidt, S. P.; Dixon, B. G., *J. Phys. Chem.* **1980**, *84* (14), 1841-1843.
10. Zaugg, W. S., *J. Bio. Chem.* **1964**, *239* (11), 3964-3970.
11. Zimmer, K.; Hoppmeier, M.; Schweig, A., *Chem. Phys. Lett.* **1998**, *293* (5-6), 366-370.
12. Pignataro, B.; Fragalà, M. E.; Puglisi, O., *Nucl. Instr. Meth. Phys. Res.* **1997**, *131* (1-4), 141-148.
13. Wenkin, M.; Devillers, M.; Tinant, B.; Declercq, J.-P., *Inorg. Chim. Acta.* **1997**, *258* (1), 113-118.
14. Chao, S.; Lu, Z.; Bai, Z.; Cui, Q.; Qiao, J.; Yang, Z.; Yang, L., *International Journal of Electrochemical Science* **2013**, *8*, 8786-8799.